

# Novel Broadband Dielectric Resonator Antennas Fed Through Double-Bowtie-Slot Excitation Scheme

G. Almpanis, C. Fumeaux, and R. Vahldieck

Swiss Federal Institute of Technology (ETH Zurich)  
 Laboratory for Electromagnetic Fields & Microwave Electronics (IFH)  
 E-mail: almpanis@ifh.ee.ethz.ch

**Abstract** — This paper discusses the concept and the realization of novel wideband dielectric resonator antennas (DRAs), in which a dielectric cylinder or parallelepiped are fed from a microstrip line through two parallel bowtie-slots. The concept of partial independence of the slot modes from the dielectric resonator mode is exploited in such a way that the resonances of the slot modes and of the DRA are designed to occur at different frequencies. As a result, the bandwidth of the DRA is significantly improved, while stability in the radiation patterns and low cross-polarization are maintained. Finally, a study is performed concerning the influence of the gap between the dielectric resonator and the ground plane upon the overall performance of the DRA. Comparison of the results from a commercial software tool (HFSS<sup>®</sup>) and from the Finite-Volume Time-Domain (FVTD) method is made.

**Index Terms** — Dielectric resonator antenna, slot-coupling, wideband antennas, bowtie slots, gap, FVTD.

## I. INTRODUCTION

The demand for wireless communications in the lower GHz range is rising dramatically due to the public's need for mobility and internet connectivity at flexible locations. Dielectric resonator antennas (DRAs) [1] are very attractive candidates for such applications, because of their high radiation efficiency, low dissipation loss and small size. Other inherent advantages include the ease of excitation, the low fabrication cost and the large bandwidth compared to a patch antenna. For instance, a DRA of dielectric permittivity  $\epsilon_r = 10$  has an impedance bandwidth of around 10%, which is wide enough for a number of applications. However, for multiband applications wider bandwidths are always of interest and therefore various bandwidth enhancement techniques have been the focus of many DRA investigations.

Most of the bandwidth enhancement techniques involve complicated structures for the dielectric resonator such as stacked DRAs [2], [3], [4], parasitic elements [5], [6], or non-canonical geometries [7], [8]. In most of these cases the manufacturing difficulty and hence the cost increases. To eliminate this problem, this paper

introduces a simple but effective method to broaden the DRA bandwidth without adding manufacturing difficulties. In this solution, a microstrip line couples energy to a dielectric resonator through two parallel bowtie-slots. The advantage of the design proposed in Figure 1 lies in the weak coupling of the dielectric resonator mode to the slot modes [9]. Therefore, the modes can be independently designed in such a way, that the resonant frequencies are sufficiently separated from one another and, as a result, the impedance bandwidth increases. Moreover, the polarization and the radiation patterns of the DRA are maintained, since the slot modes and the fundamental modes of either the cylindrical or the rectangular dielectric resonator have similar radiation characteristics.

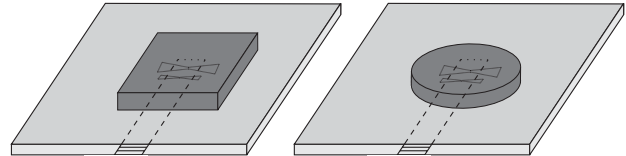


Fig. 1. Proposed antenna geometry.

The design procedure for a double-bowtie-slot-coupled DRA is described in Section II. The validity and repeatability of the design process are demonstrated in Sections III and IV, where two individual cases are considered. The first case involves a simple cylindrical dielectric resonator (DR) that is fed by the double-bowtie-slot excitation scheme, while in the second case the disc is replaced by a dielectric parallelepiped. Simulation and experimental results are shown, in order to prove the initial hypothesis. Finally, a discussion is made in Section V about the effect of a gap. Simulation and experimental results are shown, in order to prove the initial hypothesis. Finally, a discussion is made in Section V about the effect of a gap between the dielectric resonator and the ground plane of the microstrip line.

## II. DESIGN CONCEPT

The design of a dielectric resonator fed from a microstrip line through two parallel bowtie-slots is a straightforward procedure, if the concept of the partial independence of the DR mode from the slot modes is taken into consideration. Therefore, the design process can be separated into three main steps.

In the first step, the two bowtie slots are designed to be resonant at nearby frequencies  $f_1$  and  $f_2$ . To that end, the structure depicted in Figure 2 is simulated assuming a flat dielectric superstrate structure (permittivity  $\epsilon_{rd}$ ). To that end, the structure depicted in Figure 2 is simulated assuming a flat dielectric superstrate structure (permittivity  $\epsilon_{rd}$  and height  $h$ ) on top of the slots and infinitely extended in the x-y direction. This allows the computationally efficient use of the commercial software tool Ansoft Designer<sup>®</sup> (Method of Moments). The bowtie slots with lengths  $L_{s1}$ ,  $L_{s2}$  and widths  $W_{s1}$ ,  $W_{s2}$  are etched into the groundplane of a microstrip line, which is a 50  $\Omega$  line of width  $W_m$ . The distances from the centers of the two slots to the open end of the microstrip line are  $P_1$  and  $P_2$ , respectively, so that good impedance matching can be ensured.

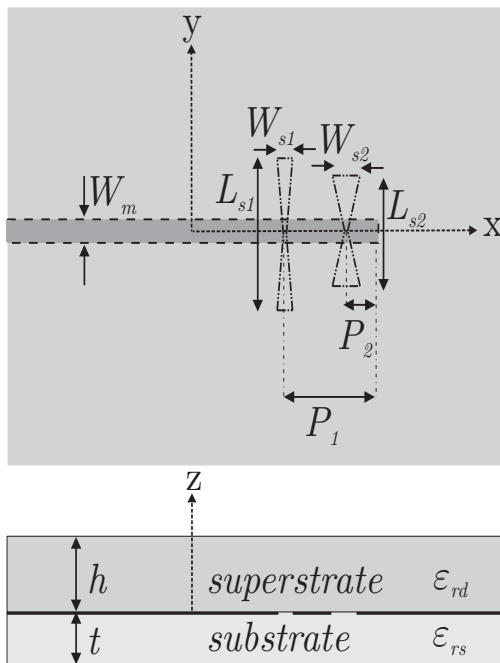


Fig. 2. Schematic of the structure with the bowtie-slots between a sub- and a superstrate.

With reference to Figure 2, the parameters that determine the frequency of resonance for the bowtie-slots are primarily the permittivity of sub- and superstrate,  $\epsilon_{rs}$  and  $\epsilon_{rd}$ , respectively, as well as the slot lengths  $L_{s1}$  and  $L_{s2}$ . The widths  $W_{s1}$  and  $W_{s2}$  (or the flare angles of the

bowties) are primarily used as matching parameters for the two slots, as well as to further increase their bandwidth [10].

The second step involves the design of the dielectric resonator. For dielectric resonators of a canonical shape like a cylinder or a parallelepiped, the literature offers us closed-form expressions for the resonant frequency of their fundamental modes [11]. Therefore, for a DR of the same permittivity  $\epsilon_{rd}$  and height  $h$  as that of the superstrate in Figure 2, the other dimensions (radius for the cylinder, length and width for the parallelepiped) are tuned in order to achieve a resonant frequency  $f_3$  for the DR, which is nearby, but larger than the frequencies  $f_1$  and  $f_2$ .

In the third step, the feeding scheme from the first step is combined with the DR designed in the second step. To do so, the feed design of Figure 2 is kept unchanged, but the lateral substrate dimensions are made finite and the superstrate is replaced by the DR, whose dimensions and permittivity were determined during the second step. The final structure, which is depicted in Figure 1, is fine-tuned, so that its impedance bandwidth is further enhanced. This optimization involves primarily the stub lengths  $P_1$  and  $P_2$ , the flare angles of the bowties as well as the position of the dielectric resonator center relative to the center line of the feeding microstrip. Since the structure is no longer infinitely extended in x- and y-direction, all the simulations in this last step are performed with Ansoft HFSS<sup>®</sup> (Finite Elements Method).

It should be emphasized that the mutual coupling of the two slots in parallel configuration may affect the radiation patterns of the DRA. The two slots in parallel point the beam at an angle different from the broadside direction. To achieve a broadside radiation pattern of the DRA, two methods can be used. First, the distance between the two slots can be further decreased with respect to the wavelength of operation. Second, shifting the center of the DR along the line connecting the slot centers does not only influence the matching, but can also affect the direction of maximum radiation. Obviously, the dielectric resonator serves as a dielectric loading for higher front-to-back ratio, but most importantly, it helps form the radiation patterns generated by the feed.

## III. DOUBLE BOWTIE-SLOT-COUPLED CYLINDRICAL DRA

For operation of the DRA in the 5.0 GHz – 6.5 GHz range using a simple dielectric cylinder, the aforementioned procedure results in an antenna geometry, as illustrated in Fig. 3. The cylindrical DRA is made from Rogers TMM<sup>®</sup> 10i laminate, with dielectric permittivity  $\epsilon_{rd} = 9.8$ , height  $h = 4.5$  mm, and radius  $r = 12$  mm. The dielectric disc lies on top of the two bowtie slots, which have dimensions  $L_{s1} = 7.9$  mm,  $L_{s2} = 6$  mm,  $W_{s1} = 0.58$

mm,  $W_{s2} = 2.02$  mm, while their width at the center is  $W_{c1} = W_{c2} = 0.3$  mm. The center of the cylindrical DR is placed at a position  $P = 3.1$  mm from the open end of the microstrip line. The width of the microstrip line is  $W_m = 2.4$  mm and its open end is at distances  $P_1 = 4.1$  mm and  $P_2 = 2.7$  mm from the slot centers. Finally, the Duroid substrate's permittivity is  $\epsilon_{rs} = 2.2$ , its thickness is  $t = 0.7874$  mm and its dimensions are  $100 \text{ mm} \times 100 \text{ mm}$ .

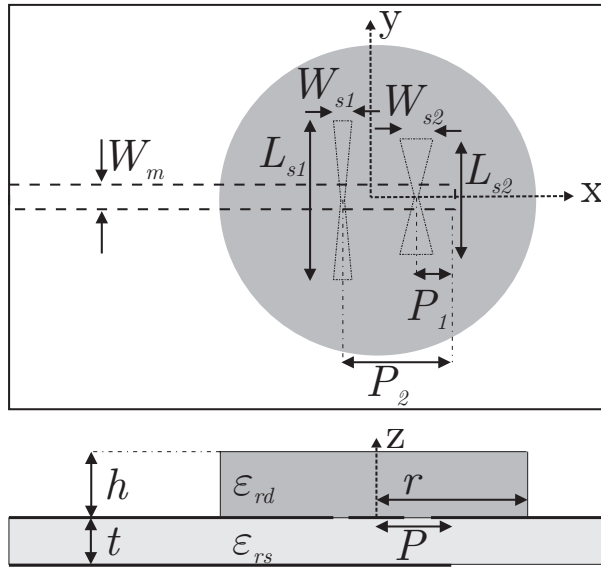


Fig. 3. Schematic of the double-bowtie-slot-coupled cylindrical DRA.

According to the specifications given above, an antenna prototype was manufactured and measured. The measured and simulated return loss of the double-bowtie-slot-coupled DRA is illustrated in Figure 4. An experimental impedance bandwidth of 33 per cent is obtained, a very satisfying value for a structure with a single cylindrical DRA. The small discrepancy between simulated and measured results is most probably caused by the gap between the ground plane and the DR. A more extensive discussion on this subject is made in Section V.

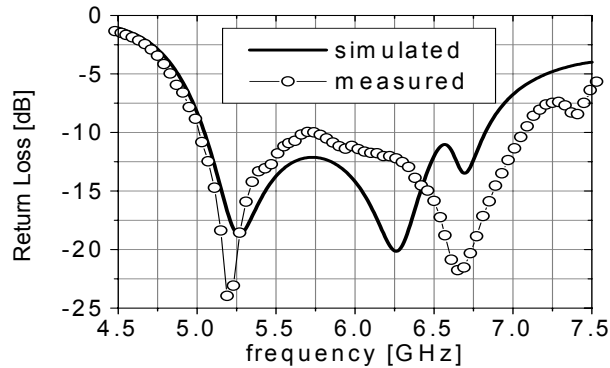


Fig. 4. Measured and simulated Return Loss of the cylindrical DRA as a function of frequency.

To further illustrate the excitation of the three modes in the proposed scheme, the simulated real and imaginary parts of the impedance are depicted in Figure 5. The two slot modes are excited at 5.6 GHz and 6.5 GHz, while the fundamental  $\text{HEM}_{110}$  mode of the cylindrical DR is at 6.75 GHz. This statement can be further substantiated by looking at the real and imaginary parts of the input impedance (Figure 6) of the infinitely extended superstrate structure depicted in Figure 2. In this case, the infinite superstrate plays the role of a dielectric loading but does not excite any resonant modes. Therefore, only the two slot modes are excited, while the presence of the dielectric loading improves the front-to-back ratio. Figure 6 proves the aforementioned hypothesis, since only two modes are observed: one at 5.65 GHz and one at 6.7 GHz. A comparison between Figures 5 and 6 clearly associates the third mode (indicated by the local maximum of the real part of the impedance) in Fig. 5 with the DR mode. It is worth mentioning that according to the simulations performed, the replacement of the superstrate by the DR slightly shifts the resonant slot modes to lower frequencies, due to the lowering of the effective permittivity  $\epsilon_{eff}$  for the slots.

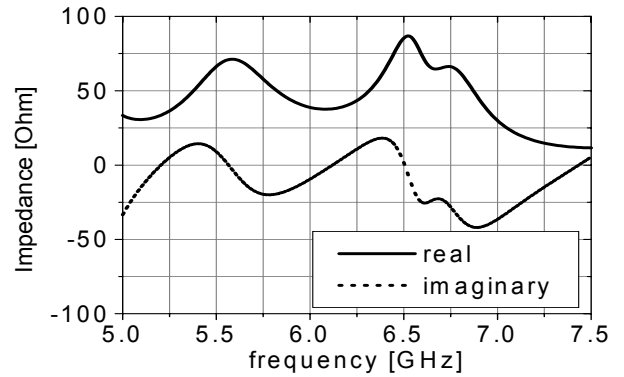


Fig. 5. Real and imaginary impedance of the structure with two bowtie-slots and the cylindrical DRA on top.

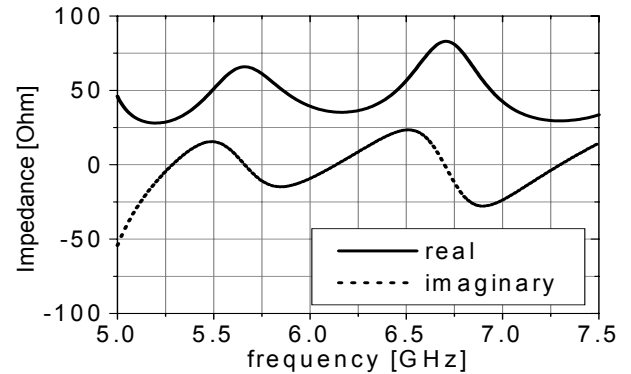


Fig. 6. Real and imaginary impedance of the structure with two bowtie-slots and a superstrate (no DRA).

The measured radiation patterns (parallel and cross polarization) are depicted in Figures 7, 8, 9 at frequencies 5.2 GHz, 6.25 GHz, and 6.7 GHz, respectively. As expected, the polarization remains reasonably pure for a wide angle range and the gain in the broadside direction is stable at around 3.5 dBi. In addition to that, the shift of directivity to an off-broadside angle, caused by the slot array, has been cancelled through the optimization of the distance between the slots and the position of the center of the dielectric disc. Therefore, stable radiation patterns are achieved.

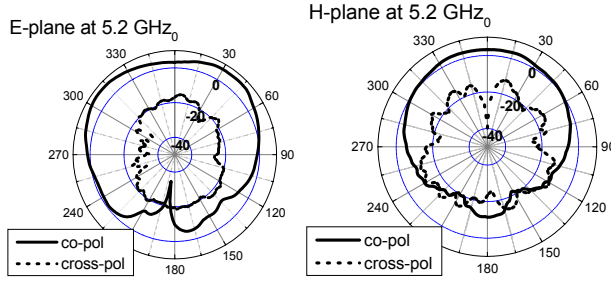


Fig. 7. Measured radiation patterns of the cylindrical DRA at 5.2 GHz.

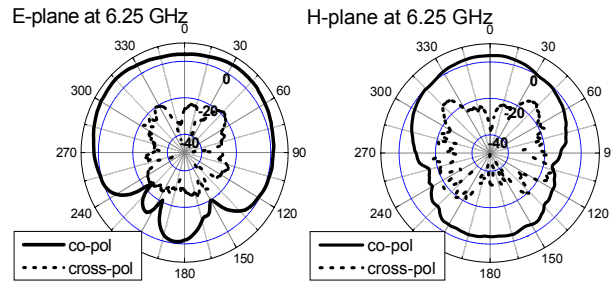


Fig. 8. Measured radiation patterns of the cylindrical DRA at 6.25 GHz.

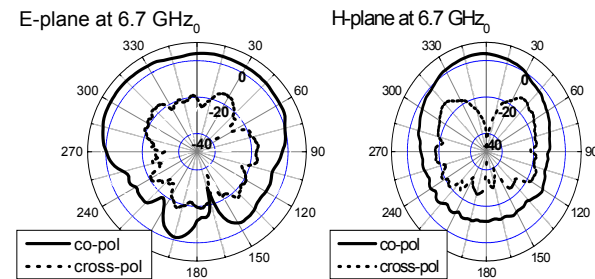


Fig. 9. Measured radiation patterns of the cylindrical DRA at 6.7 GHz.

#### IV. DOUBLE BOWTIE-SLOT-COUPLED RECTANGULAR DRA

The general validity of the proposed design procedure is further substantiated by the application of the same concept to the case of a rectangular DR fed by two

parallel bowtie slots. It should be noted that the choice of the cylindrical and the rectangular dielectric resonator was made based on two criteria: the presence of closed formed expressions for the determination of the frequencies of the resonant modes and the ease of fabrication.

For the same frequency range of operation, the feed geometry and the dimensions of the various components are kept unchanged from the cylindrical DRA configuration. The sole difference is obviously the dielectric resonator, which is now a parallelepiped made from Rogers TMM<sup>®</sup> 10i laminate of dielectric permittivity. The sole difference is obviously the dielectric resonator, which is now a parallelepiped made from Rogers TMM<sup>®</sup> 10i laminate of dielectric permittivity  $\epsilon_{rd} = 9.8$  with dimensions  $a = d = 20.5$  mm and  $h = 4.5$  mm. For better matching and radiation patterns, the rectangular DR is centered at a distance  $P' = 3.6$  mm from the open end of the microstrip line, and displaced by distance  $\Delta y = 1.2$  mm from the microstrip's center line.

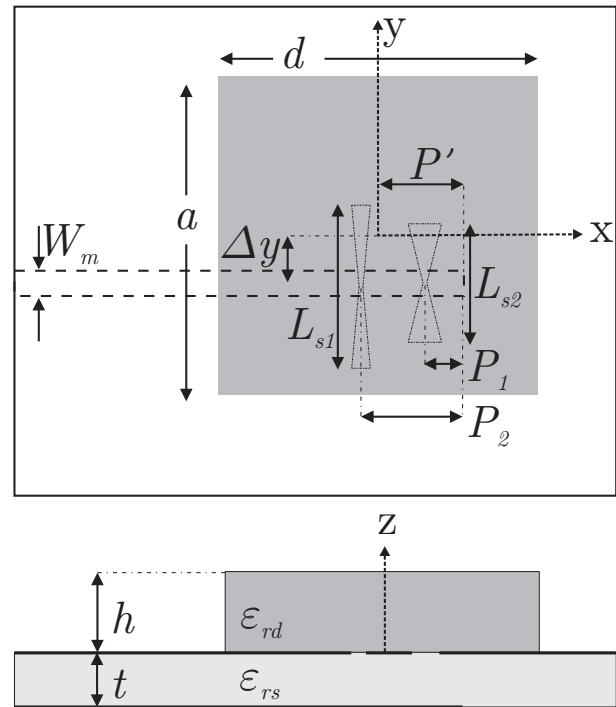


Fig. 10. Schematic of the double-bowtie-slot-coupled rectangular DRA.

The DRA was manufactured according to the geometry depicted in Figure 10. Figure 11 shows the resulting return loss and a measured bandwidth of more than 37%. Good agreement is obtained between simulation and experiment.

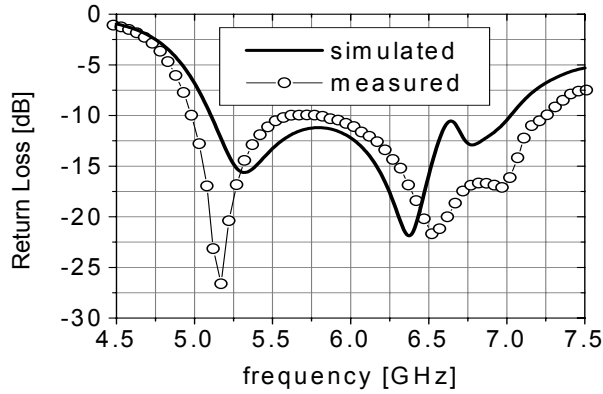


Fig. 11. Measured and simulated Return Loss of the rectangular DRA as a function of frequency.

Finally, the radiation patterns (parallel and cross polarization) of the rectangular DRA are shown in Figures 12, 13, 14 at frequencies 5.15 GHz, 6.5 GHz, and 6.95 GHz, respectively. Just like in the cylindrical configuration, stable radiation patterns are achieved. It is important to note here that if a rectangular (not a square) DR had been used ( $a \neq d$  in Figure 10), the polarization purity would have been improved. This is due to the fact that the  $TE_{111}^x$  mode would be resonant at a different frequency compared to the  $TE_{111}^y$  mode and therefore the polarization at the frequency of the  $TE_{111}^y$  mode would not be distorted by the orthogonal resonant mode.

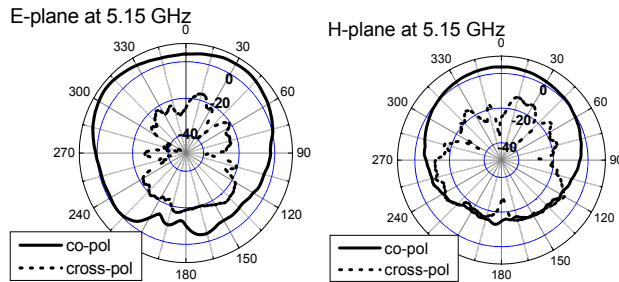


Fig. 12. Measured radiation patterns of the rectangular DRA at 5.15 GHz.

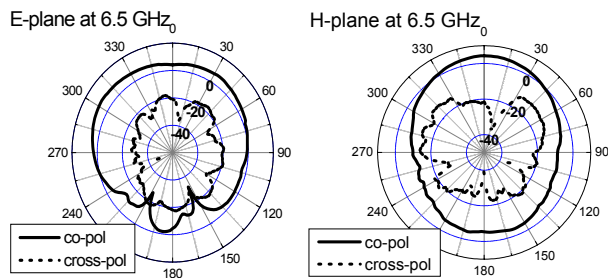


Fig. 13. Measured radiation patterns of the rectangular DRA at 6.5 GHz.

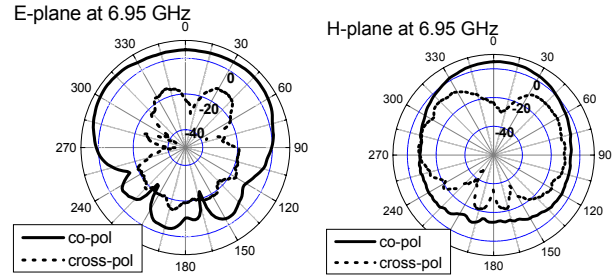


Fig. 14. Measured radiation patterns of the rectangular DRA at 6.95 GHz.

## V. EFFECT OF THE GAP BETWEEN THE GROUNDPLANE AND THE DIELECTRIC RESONATOR

The comparison between the HFSS simulations and the measured data for the return loss of the fabricated DRAs reveals a reasonably good agreement (Figures 4 and 11). It demonstrates an accurate numerical design of the operational bandwidth, despite the fact that observed S11 resonances are slightly shifted. The discrepancies between simulations and measurements can be partly explained by imperfections of the realized prototypes. Fabrication imperfections relevant to probe-fed DRAs have been discussed in [12] and [13]. In the present case of a slot-fed DRA, a major physical source of error consists in a gap between the dielectric resonator and the metallic ground plane. For the prototypes fabricated in the frame of the present investigations, the dielectric resonator adheres to the ground plane using a thin layer of Vaseline (Fig. 15). This allows easy variation of the relative location of the DR with respect to the feed circuit, for testing purposes. In addition, this way of attaching the DR presented the advantage of allowing a convenient reuse of the same feeding circuit with various dielectric resonators. This adhesion layer might be replaced by dielectric glue in future fabrication runs.

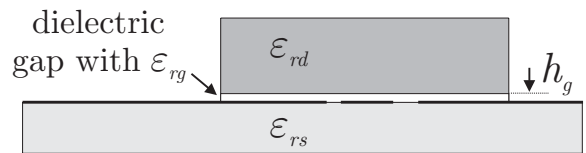


Fig. 15. Schematic showing the characteristics of dielectric gap between the DR and the ground plane.

The present section presents a numerical study of the effect of this Vaseline-filled gap for the case of the double-bow-tie slot fed cylindrical DRA. A full simulation of the device including the dielectric gap faces two main difficulties:

First, the thickness  $h_g$  of the gap is not well known. A constant gap thickness  $h_g$  of a few tens of microns is assumed. More precise information is not available, neither in the form of an average gap size, nor regarding typical gap variations under the surface of the DR. The dielectric permittivity  $\epsilon_{rg}$  of the Vaseline is estimated to take a value between 2 and 3.

Second, simulating a gap with a thickness below 50  $\mu\text{m}$  in the lower GHz frequency range is a very challenging task for general-purpose electromagnetic simulation tools, since the gap thickness is in the order of  $\lambda_0 / 500$  or smaller.

The latter problem is best solved by using a strongly inhomogeneous mesh to resolve the gap. This has been done with the commercial code HFSS<sup>®</sup> and, for comparison, also with an in-house written code based on the Finite-Volume Time-Domain method. Both methods make use of tetrahedral meshes, which permit rapid variations in cell sizes to accommodate fine structural details equally well as the free space surrounding the DR. Apart from this common feature, the two methods differ greatly, and some characteristics relevant to the present simulation are shortly described in the following:

a) HFSS is based on the Finite-Element method in the frequency domain. The resolution of the gap requires a dramatic increase in the number of cells. The limitation in the capability to solve the present problem arises since the memory load increases faster than linearly with the number of unknowns, leading to an explosion of the memory costs. In the present study, the resolution of thin dielectric gaps in HFSS simulations required at times more than 10 GB of memory.

b) The FVTD method [14], [15] is a time-domain method that can be used in any polyhedral discretization. It is therefore characterized by a large geometrical flexibility, e.g., when applied in a tetrahedral mesh. Applications of the method to DRAs have been presented previously in [13] and [16]. The second of those references in particular shows the simulation of a slot-fed DRA. In the present case (as for HFSS), the resolution of the dielectric gap between the ground plane and the DR also increases dramatically the number of cells in the tetrahedral mesh. However, because of only a linear increase of the memory with the number of unknowns, the memory cost remains at a level around 1 GB, compatible for use on a standard PC. The limitation in the capability of the program to solve the dielectric gap problem is more due to the CPU time required to achieve convergence of the results in this resonant structure. Even when using a local-time stepping technique [17], the efficiency of the scheme is not dramatically increased, since tiny cells, which are required for the gap resolution, represent a very large percentage of the total number of cells. Therefore, simulations of a DRA in the presence of

very thin gaps requires several days of computations, limiting the simulation capabilities.

Because of the incomplete knowledge of the gap properties, and because of the limitation of both tools chosen for the numerical simulation, the present analysis must be interpreted in a qualitative manner, as a demonstration of the potential effects of a gap between the dielectric and the ground plane. Several configurations of Vaseline-filled gaps have been tested with both tools in the case of the cylindrical DR fed by double bow-tie slots (presented in Sect. III). The results are shown in Figure 16 for HFSS and Figure 17 for FVTD. In both cases, the dielectric gap is of height  $h_g = 30 \mu\text{m}$  and of dielectric permittivity  $\epsilon_{rg} = 2.7$ . Both figures include the simulated return loss with and without dielectric gap, as well as the measured data for comparison. From those graphs, it is observed that without the gap, both simulation tools represent the -10 dB bandwidth of operation with reasonable accuracy, although slight differences occur. In addition, it is observed that the introduction of a thin dielectric gap between the DR and the ground plane has a sensible effect on the simulated performance. This effect is qualitatively very similar for both numerical tools and supports our assumption about the effect of the small gaps on the return loss. A more precise match to simulation is not expected, considering that the modeling of the dielectric gap is at the limit of the capabilities of both tools and that the real characteristics of the dielectric gap are unknown.

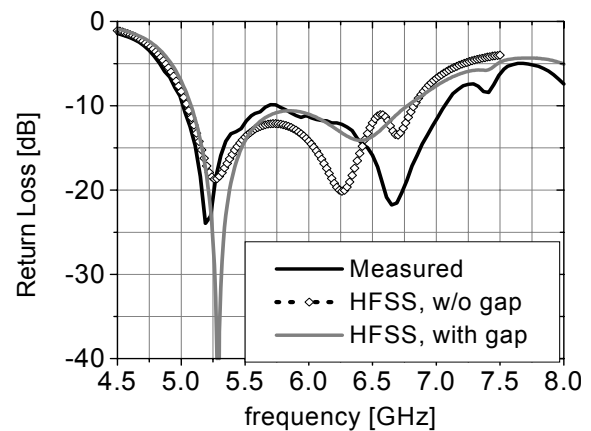


Fig. 16. HFSS simulations of the return loss for the cylindrical DRA with and without dielectric gap (thickness  $h_g = 30 \mu\text{m}$ ,  $\epsilon_{rg} = 2.7$ ). The curves are compared to measured data.

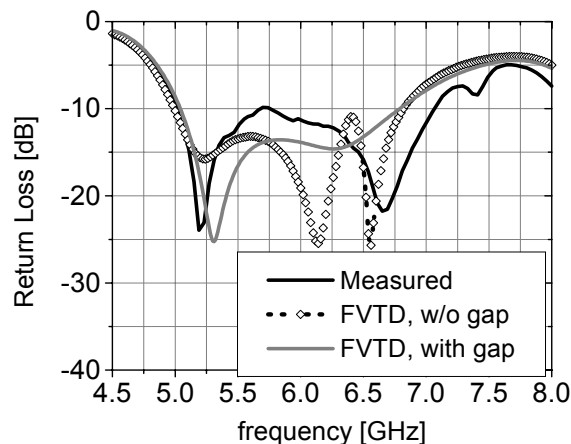


Fig. 17. FVTD simulations of the return loss for the cylindrical DRA with and without dielectric gap (thickness  $h_g$ ). FVTD simulations of the return loss for the cylindrical DRA with and without dielectric gap (thickness  $h_g = 30 \mu\text{m}$ ,  $\epsilon_{rg} = 2.7$ ). The curves are compared to measured data.

## VI. CONCLUSION

It was shown that the resonances of a 2-element array of bowtie-slots and a dielectric resonator can be combined for bandwidth enlargement. Novel double-bowtie-slot-coupled DRA designs were proposed with more than 30 % bandwidth, 3.5 dBi gain in the broadside direction, and stable radiation patterns and polarization. The effect of the gap between the dielectric resonator and the ground plane of the microstrip line has been discussed.

## ACKNOWLEDGMENT

The authors would like to acknowledge the valuable support from H.-R. Benedickter. The authors are also grateful to M. Lanz for fabricating the feeding structure. This work was supported by ETH Research Grant TH-38/04-1.

## REFERENCES

[1] S. A. Long, M. W. McAllister, and L. C. Shen, "The resonant cylindrical dielectric cavity antenna," *IEEE Trans. Antennas Propagation*, Vol. 31, No. 3, pp. 406 - 412, May 1983.

[2] A. Petosa, A. Ittipiboon, Y. M. M. Antar, D. Roscoe, and M. Cuhaci, "Recent advances in dielectric-resonator antenna technology," *IEEE Antennas and Propagation Magazine*, Vol. 40, No. 3, pp. 35 - 48, June 1998.

[3] A. A. Kishk, B. Ahn and D. Kajfez, "Broadband stacked dielectric resonator antennas," *Electronics Letters*, Vol. 25, No. 18, pp. 1232 - 1233, Aug. 1989.

[4] K. W. Leung, K.Y. Chow, K.M. Luk, and E. K. N. Yung, "Offset dual-disk dielectric resonator antenna of very high permittivity," *Electronics Letters*, Vol. 32, No. 22, pp. 2038 - 2039, Oct. 1996.

[5] A. Laisne, R. Gillard and G. Piton, "Circularly polarized dielectric resonator antenna with metallic strip," *Electronics Letters*, Vol. 38, No. 3, pp. 106 - 107, Jan. 2002.

[6] B. Li and K. W. Leung, "Strip-Fed Rectangular Dielectric Resonator Antennas With/Without a Parasitic Patch," *IEEE Trans. Antennas Propagation*, Vol. 53, No. 7, pp. 2200 - 2207, July 2005.

[7] A. A. Kishk, Y. Yan, A. W. Glisson, "Conical dielectric resonator antennas for wide-band applications," *IEEE Trans. Antennas Propagation*, Vol. 50, No. 4, pp. 469 - 474, April 2002.

[8] A. Ittipiboon, A. Petosa, D. Roscoe and M. Cuhaci, "An Investigation of a Novel Broadband Dielectric Resonator Antenna," *IEEE International Symposium on Antennas and Propagation Digest*, Baltimore, MA, pp.2038-2041, June 1996.

[9] A. Buerkle, K. Sarabandi and H. Mosallaei, "Compact Slot and Dielectric Resonator Antenna With Dual-Resonance, Broadband Characteristics," *IEEE Trans. Antennas Propagation*, Vol. 53, No. 3, pp. 1020 - 1027, March 2005.

[10] G. Almpanis, C. Fumeaux, and R. Vahldieck, "Double-Bowtie-Slot-Coupled DRA for Enhanced Bandwidth," *22nd Annual Review of Progress in Applied Computational Electromagnetics*, ACES, Miami, FL, USA, pp. 812-818, March 2006.

[11] K. M. Luk and K. W. Leung, "Dielectric Resonator Antennas", Research Studies Press, Baldock, England, 2003.

[12] G.P. Junker, A.A. Kishk, A.W. Glisson and D. Kajfez, "Effect of fabrication imperfections for ground-plane-backed dielectric-resonator antennas," *IEEE Trans. Antennas Propagation*, Vol. 37, No. 1, pp. 40-47, Feb. 1995.

[13] C. Fumeaux, D. Baumann and R. Vahldieck, "Advanced FVTD simulation of dielectric resonator antennas and feed structures," *ACES Journal*, Vol. 19, No. 3, pp. 155-164, Nov. 2004.

[14] V. Shankar, A.H. Mohammadian and W.F. Hall, "A time-domain, finite-volume treatment for the Maxwell equations," *Electromagnetics*, Vol. 10, pp. 127-145, 1990.

[15] P. Bonnet, X. Ferrieres, B.L. Michielsen, P. Klotz and J.L. Roumiguieres, "Finite-Volume Time Domain Method", Chapter 9 in *Time domain electromagnetics*, edited by S.M. Rao, Academic Press, San Diego, 1999.

- [16] D. Baumann, C. Fumeaux, G. Almpanis and R. Vahldieck, "Microstrip port definition in FVTD and application to slot-fed dielectric resonator antennas," *22<sup>nd</sup> Annual Review of Progress in Applied Computational Electromagnetics, ACES*, Miami, FL, USA, pp. 787-794, March 2006.
- [17] C. Fumeaux, D. Baumann, P. Leuchtmann and R. Vahldieck, "A generalized local time-step scheme for efficient FVTD simulations in strongly inhomogeneous meshes," *IEEE Trans. Microwave Theory and Techniques*, Vol. 52, No. 3, pp. 1067-1076, March 2004.



**Georgios Almpanis** received the Dipl. Ing. degree in electrical and computer engineering from the National Technical University of Athens, Greece, in 2003, the M.Sc degree in Optics and Photonics from CREOL & FPCE, UCF, Florida, USA in 2004 and is currently working toward the Ph.D. degree at the Swiss Federal Institute of Technology (ETH)

Zürich, Zürich, Switzerland.

In the Summer of 2002 he did an internship in the Norwegian University of Science and Technology (NTNU), in Trondheim, Norway. From March to August 2003, he was a Research Scientist with the Greek Telecommunications Company, working on the field of antenna engineering. In January 2005, he joined the ETH Zürich, where he is currently with the Laboratory for Electromagnetic Field Theory and Microwave Electronics (IFH). His main research interests include dielectric resonator antennas and ultra-wideband communication systems.

Mr. Almpanis was a 3<sup>rd</sup> prize winner at the 6<sup>th</sup> European Union Contest for Young Scientists in Helsinki, Finland, in 1996. He was a recipient of a scholarship from the Fulbright Foundation for the academic year 2003-2004 and from the Gerondelis Foundation for the academic year 2004-2005.



**Christophe Fumeaux** received the Diploma and Ph.D. degrees in physics from the Swiss Federal Institute of Technology (ETH), Zurich, Switzerland, in 1992 and 1997, respectively. From 1998 to 2000, he was a Post-Doctoral Researcher involved in infrared technology with the School of Optics, University of Central Florida, Orlando. In

2000, he joined the Swiss Federal Office of Metrology, Bern, Switzerland, as a Scientific Staff Member. Since 2001, he has been a Research Associate with the Laboratory for Electromagnetic Fields and Microwave Electronics (IFH), ETH, Zürich, Switzerland. During the Fall of 2005, he was a Visiting Scientist with the Laboratory of Sciences and Materials for Electronics, and of Automatic (LASMEA), University Blaise Pascal, Clermont-Ferrand, France. His current main research

interest concerns computational electromagnetics in the time domain for numerical analysis of microwave circuits and antennas.

Dr. Fumeaux has been the chairman of the IEEE Swiss Joint Chapter on Microwave Theory and Techniques, Antennas and Propagation, and EMC since January 2006. He was the recipient of the ETH Silver Medal of Excellence for his doctoral dissertation. He was the recipient of the outstanding paper award of the Applied Computational Electromagnetics Society (ACES) in 2004.



**Ruediger Vahldieck** received the Dipl.-Ing. and the Dr.-Ing. degrees in electrical engineering from the University of Bremen, Germany, in 1980 and 1983, respectively.

He was a Postdoctoral Fellow with the University of Ottawa, Ottawa, ON, Canada, until 1986. In 1986, he joined the Department of Electrical and Computer

Engineering, University of Victoria, BC, Canada, where he became a Full Professor in 1991. During Fall and Spring of 1992 to 1993 he was a Visiting Scientist at the "Ferdinand-Braun-Institute für Hochfrequenztechnik", Berlin, Germany. In 1997, he was appointed Professor for electromagnetic field theory at the Swiss Federal Institute of Technology, Zurich, and became head of the Laboratory for Electromagnetic Fields and Microwave Electronics (IFH) in 2003. In 2005, he became President of the Research Foundation for Mobile Communications and was elected Head of the Department of Information Technology and Electrical Engineering (D-ITET), ETH Zurich. Since 1981 he has published more than 300 technical papers in books, journals and conferences. His research interests include computational electromagnetics in the general area of EMC and in particular for computer-aided design of microwave, millimeter wave and optoelectronic integrated circuits.

Dr. Vahldieck received the Outstanding Publication Award of the Institution of Electronic and Radio Engineers in 1983, the K.J. Mitra Award of the IETE (in 1996) for the best research paper in 1995, and the ACES Outstanding Paper Award in 2004. He is the Past-President of the IEEE 2000 International Zurich Seminar on Broadband Communications (IZS'2000) and since 2003 President and General Chairman of the international Zurich Symposium on Electromagnetic Compatibility (EMC Zurich). He is a member of the editorial board of the IEEE TRANSACTIONS ON MICROWAVE THEORY AND TECHNIQUES. From 2000 until 2003 he served as Associate Editor for the IEEE MICROWAVE AND WIRELESS COMPONENTS LETTERS and from July 2003 until the end of 2005 as the Editor-in Chief. Since 1992, he has been on the Technical Program Committee of the IEEE International Microwave Symposium, the MTT-S Technical Committee on Microwave Field Theory, and in 1999 on the TPC of the European Microwave Conference. From 1998 until 2003 Professor Vahldieck was the Chapter Chairman of the IEEE Swiss Joint Chapter on MTT, AP, and EMC.